

Controlling Whisker Formation in Tin-Based Solders Using Electrically Mediated Electrodeposition

H. Garich, H. McCrabb, E. J. Taylor, and M. Inman

Faraday Technology, Inc, 315 Huls Drive, Clayton, Ohio 45315, USA

The global trend to eliminate lead from electronic devices is driven by legislative and marketing pressures based on environmental, health and social concerns on the cumulative effects of lead in waste streams. Tin and tin-rich alloys are the forerunning replacements for tin-lead solders. However, pure tin electrodeposits have a tendency to form tin whiskers that may cause short-circuiting, metal vapor arcing and failure of the component. The major cause of whisker growth is thought to be compressive stress in pure tin deposits after DC plating. Faraday Technology, Inc. has developed an electrically mediated electrochemical process for depositing lead-free solders, based on non-steady state electric fields to control the deposition process and consequently the physical properties of the deposit. Results of electrically mediated tin deposits are presented and compared to DC deposits in terms of grain size, internal stress type/magnitude and surface roughness.

Introduction

The electronic industry has experienced great strides in miniaturization and higher I/O packing densities in the last couple decades, with one constant, the use of tin-lead solders to connect electronic components to the base printed circuit boards (PCBs). With legislation enforced since July 1, 2006 in the European Union (EU), namely Directive 2002/95/EC (ROHS), which places restrictions on the use of certain hazardous materials in electronic equipment, manufactures have been investigating alternatives for tin-lead solders. Pure tin has been identified as “the most promising drop-in replacement” for tin-lead solder in terms of solderability, compatibility with existing processes/assemblies, ease of process control and cost effectiveness (1). However, one of the largest problems associated with the use of pure-tin and other tin-rich lead-free alloys is a tendency to form tin whiskers, which may cause permanent and intermittent shorting, metal vapor arcing and ultimately product failure. For example, Boeing reported failure of a processor due to tin whiskers, resulting in the complete loss of a \$200 million communication satellite (1).

While the causes and the mechanisms of whisker formation is unknown, several contributing factors have been identified and include: recrystallization, environmental conditions, and presence of stresses in the deposit. Stresses in the deposit may result from the plating process, intermetallic compound (IMC) formation at the interface between the substrate and the deposit, mechanical loading, surface damage of the substrate and/or deposit, and mismatch of the coefficient of thermal expansion between the substrate and deposit (2). It is generally recognized that compressive stresses in the

tin deposits promote whisker formation, presumably due to the interdiffusion processes that result in IMC formation; IMC formation results in specific volume changes, altering the lattice spacing, which results in compression of the tin layer and tension to the substrate (1). It is speculated that tin whiskers then grow as a relief mechanism for the compressive stress in the tin deposit (3,4).

Several mitigation techniques have been proposed for the elimination of tin whisker growth, although there is a great deal of contradictory data in the literature and no single standard method of testing. Some of the mitigation strategies being investigated include: 1) use of matte or low stress tin finishes, 2) use of an underlayer (such as Ni, Ni-Pd, and Ni-Pd-Au), 3) use of thick tin platings, 4) application of a post-heat treatment such as reflowing or annealing, 5) use of a conformal coating, and 6) minimization of compressive loads on the plated tin surface (1). Another mitigation strategy is the elimination of pure tin platings, although the other mitigation strategies have associated disadvantages in addition to adding complexity to the manufacturing process. Faraday Technology is investigating mitigation of whiskers in pure tin electrodeposits through precise control of the properties of the tin electrodeposit through control of the plating process with the use of electrically mediated waveforms.

Electrically Mediated Electrolysis

For deposition, the electrically mediated waveform (Figure 1) consists of a cathodic pulse current density (i_c), a cathodic on time, (t_c), and may be coupled with an anodic pulse current density (i_a) with an anodic on time (t_a) and/or an off time (t_o). The sum of the cathodic and anodic on-times and the off time is the period, (T) of the modulation and the inverse of the period is the frequency. The cathodic (g_c) and anodic (g_a) duty cycles are the ratios of the respective on-times to the period. The average current density or net electrodeposition rate is given by:

$$\text{Electrodeposition Rate} = i_c \gamma_c - i_a \gamma_a \quad [1]$$

Just as there are infinite combinations of height, width, and length to obtain a given volume, electrically mediated electrolysis may utilize unlimited combinations of peak current densities, duty cycles, and frequencies to obtain a given electrodeposition rate. It should be noted that the cathodic on-time, anodic on-time and off-time, as well as the cathodic and anodic peak current densities are additional parameters available to control the electroplating process compared to conventionally used direct current (DC) plating. In DC plating, the cathodic current is turned on and held for the duration of the plating process.

Control of Grain Size with Electrically Mediated Electrolysis. Grain size in electrodeposits is a function of the crystallization mechanism, by which adatoms are incorporated into the crystal lattice. This mechanism has two distinct paths that are in competition: growth on previously deposited crystals or nucleation of new crystals. As

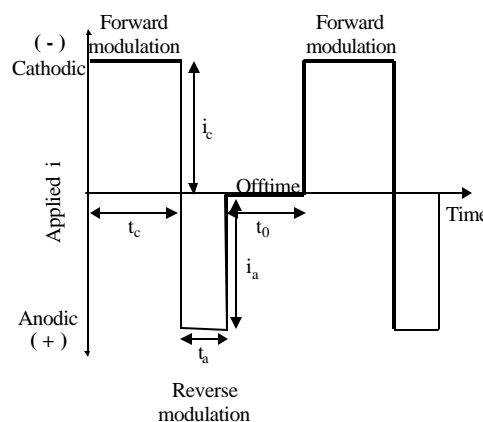


Figure 1. An example of an electrically mediated waveform.

ions enter the electrified interface between the solution and the cathode, a charge transfer reaction results in the formation of adatoms. Crystal growth dominates when there is a low concentration of adatoms under the conditions of high surface diffusion rates and low overpotentials, while nucleation is driven by high adatom concentrations, low surface diffusion rates and high overpotentials. Since electrically mediated deposition often utilizes peak cathodic current densities much higher than DC current densities, the concentration of adatoms on the surface is higher than during DC deposition, favoring nucleation and a finer grained structure. Similarly, higher overpotentials are often realized in electrically mediated electrolysis, as compared to DC electrolysis, providing a greater amount of energy available for nucleation. The crystallization overpotential h can be expressed in the following equation:

$$h = \frac{RT}{nF} \ln\left(\frac{C_{ad}^o}{C_{ad}}\right) \quad [2]$$

where, C_{ad}^o is the adatom concentration, C_{ad} is the maximum adatom concentration, R is the gas constant, T is the temperature, n is the number of electrons transferred in the reaction, and F is the Faraday constant. The nucleation rate (v) is given by the following equation:

$$v = k_1 \exp(-k_2/|\eta|) \quad [3]$$

where k_1 is a proportionality constant and k_2 is related to the amount of energy needed for the two-dimensional nucleation, and is clearly dependent upon the overpotential (5). More specifically, the nucleation rate increases exponentially with increasing overpotential, as defined in Equation 3. The rate of nucleation as a function of time is given by:

$$N = \frac{i}{kt^3} \quad [4]$$

where N is the number of nucleation sites, i is the current density corresponding to the nucleation rate, k is a nucleation constant, and t is the time. As specified by Equation 4, the activation of the nucleation sites is therefore directly proportional to the current density and inversely proportional to the cube of the time. By controlling the peak current (or voltage) of the electrically mediated waveform, the system may be driven towards either nucleation or grain growth. Control of grain size in pure tin plating is important as small grains (<1 μm , bright tin deposits) have a higher tendency to form whiskers, as they are thermodynamically less stable than larger grains (1-8 μm), initiating a recrystallization mechanism that results in whisker formation (6). In addition, diffusion is enhanced through the presence of a higher number of grain boundaries, resulting in a higher rate of IMC formation. Thus, the current work targeted 1-8 μm size grains.

Control of Internal Stresses with Electrically Mediated Electrolysis. Knodler measured the mechanical properties of both pulsed and DC plated precious metal alloy deposits, and stated “DC deposits are known to be highly stressed”(7). Knodler demonstrated that through the use of pulse plating, the stresses in the deposit could be drastically reduced, as compared to deposits from DC plating. In the current work, this concept is expanded, as careful consideration is placed on the individual components of the waveform, i.e. an electrically mediated approach, and their effect on the resulting stress in the tin deposits. Since the general consensus is that whiskers form due to

compressive stress in the deposits, the build up of different types of stresses through the use of waveform sequencing to eliminate the possibility of whisker formation was investigated. For example, the propensity of whisker formation from a deposit that consists of alternating compressive and tensile stress layers was investigated and evaluated through temperature cycling tests.

Experimental

Qualification and Characterization Tests

All tin deposition work reported was conducted using a rotating disc electrode (RDE) apparatus. A photograph of the RDE apparatus, including RDE holder and soluble pure tin anode is given as Figure 2; a multipurpose polycarbonate tank (4.7 L capacity) functioned as the plating tank. Deposition was achieved with a Dynatronix Model DPR-20-5-10 rectifier capable of delivering both electrically mediated and DC waveforms. The electrolyte used for plating consisted of 240 mL/L methanesulfonic acid (MSA), 107 g/L tin (II) methanesulfonate and 300 ppm Triton-X. The temperature of the plating bath was held constant at 37 (± 1) °C for all deposition experiments.

The hydrodynamics of the system were controlled with two rotation speeds, 100 and 400 rpm. Tin was deposited with both DC and electrically mediated waveforms. The waveforms were selected to compare the physical properties of the tin deposited as a function of selected deposition parameters. More specifically, two current densities were selected, a high current density as well as a low current density. Similarly, two duty cycles and two frequencies were utilized for these experiments. Electrically mediated waveforms were either in the form of cathodic pulse followed by an off-time or in the form of a cathodic pulse followed by an anodic pulse. In this manner, four DC tests (one at high current density and one at low current density, both tested at 100 and 400 rpm), eight cathodic pulse waveform (pulsed current, PC) tests and eight cathodic-anodic pulse waveform (pulse-reverse current, PRC) tests were conducted. For each test, tin was plated to 10 μm thickness on square copper substrates (25.4-mm² x 1.64-mm thick coupons).

The deposits were then characterized in terms of surface morphology, stress, grain size and whisker formation. Scanning electron microscopy (SEM) was used to determine grain size and shape as well as surface morphology. The internal stress of each deposit was measured using x-ray diffraction (XRD) to determine the lattice constant and therefore the strain on reflecting planes due to stress in the film.

The deposits were observed after three years of aging to determine the propensity of each to grow whiskers. The coupons were stored for one and a half years in a sealed container in a water bath held at constant temperature of 34 (± 1) °C; the coupons were stored under ambient conditions for the next year and a half. Whiskers were observed

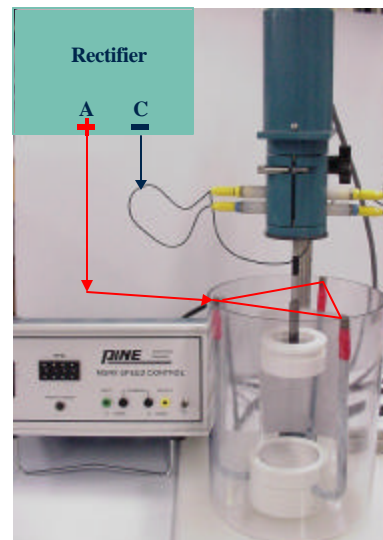


Figure 2. RDE apparatus used for tin deposition work.

and recorded with a Zeiss Compound Optical Microscope with a Video Measurement System.

Temperature Cycling Tests

The same experimental set-up, including RDE apparatus, plating electrolyte and plating temperature, was also used for coupons prepared for temperature cycling tests. However, the temperature cycling tests utilized brass substrates (25.4-mm x 12.7-mm x 1.6-mm thick coupons) with 5 μm tin deposits. Two of the brass coupons were plated together during a single plating experiment in the 25.4-mm² RDE holder, as indicated by Figure 3. In Figure 3, the plated area of the tin is represented schematically; each coupon had 200 μm^2 area of plated tin.

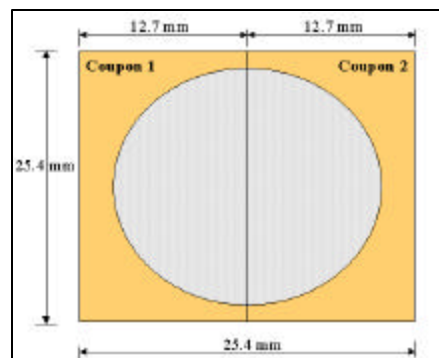


Figure 3. Schematic of plating methodology for brass coupons.

The waveforms used to prepare the brass coupons were taken from the qualification and characterization waveform matrix.

However, for temperature cycling tests, the tin deposits were stratified with type of internal stress, determined with XRD. A schematic of the graded deposits used for these tests is given in Figure 4. The stratified tin deposits were achieved by sequencing waveforms together. For instance, Coating E in Figure 4 was deposited by sequencing four distinct waveforms together to plate 1.25 μm of tin with each type of stress. It is important to note, however, that the internal stresses achieved with each waveform were measured on 10 μm tin deposits on copper substrates, not brass substrates. Therefore, the internal stress delivered by one waveform on copper may not be the same stress obtained with the same waveform on a brass substrate.

Coating A	Coating B	Coating C
Low Tensile	High Tensile	High Tensile
		Low Tensile
BRASS	BRASS	BRASS
Coating D	Coating E	Coating F
High Tensile	High Tensile	Low Tensile
Low Tensile	Low Tensile	High Tensile
Low Compressive	Low Compressive	Low Compressive
	High Compressive	High Compressive
BRASS	BRASS	BRASS

Figure 4. Schematic illustrating stratified stress coatings used for temperature cycling and high temperature/humidity storage tests.

The conditions for the temperature cycling tests are given in Table I and are set according to JESD22A121.01, "Test Method for Measuring Whisker Growth on Tin and Tin-Alloy Surface Finishes" (8). According to this standard, a total inspection area of at least 75 mm² on at least 3 coupons must be inspected for each test condition, such that on each coupon 25 mm² was inspected. These tests were conducted by the University of Maryland's CALCE Center and were carried out for 1000 cycles.

TABLE I: Testing conditions for temperature cycling tests.

Test Type	Test Conditions	Inspection Intervals	Minimum Duration
Temperature Cycling	-55 °C to 85 °C ~ 3 cycles/hour 5-10 min dwell time	500 cycles	1000 cycles

Results And Discussion

Qualification And Characterization Tests

The effect of waveform parameters was first investigated in terms of surface morphology, grain size, and internal stress type and magnitude. It was determined that the varying waveform parameters do influence the properties of the deposits obtained, indicating that the physical properties may be controlled by electrically mediated deposition as compared to DC deposition. The effect of waveform parameters on grain size is illustrated in Figure 5. Grain sizes in the range of 1-8 μm were desired for the current study. The dashed line on Figure 5 indicates that those tests above the line have 90% of their grains in the 1-8 μm range.

The internal stress of each tin deposit was measured with XRD the day after plating and six weeks after plating; the results are given in Figure 6. From Figure 6, it is obvious that the stresses in the deposit change upon aging for six weeks. Generally, the stresses in these pure tin deposits shifted to a more compressive state. It is interesting to note that the tests utilizing both a cathodic and anodic pulse (PRC tests) had less of a change, one deposit even remained in the tensile region, while the others went to zero, or slightly compressive.

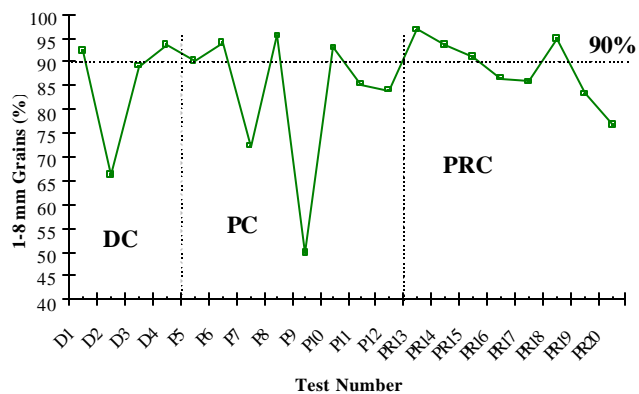


Figure 5. Plot of Percentage of Grain Sizes in the 1-8 mm Target Range as a Function of Test Conditions.

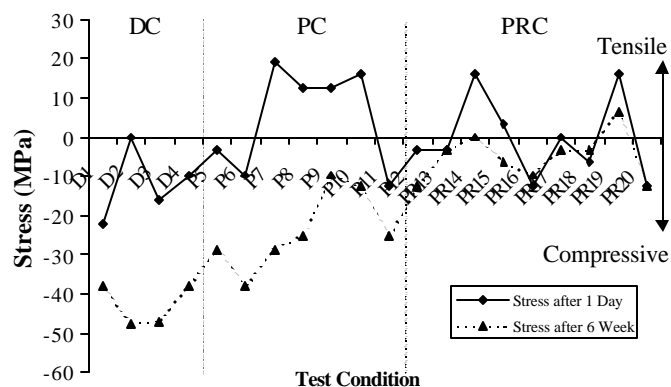


Figure 6. Internal Stress of Each Deposit, One Day after Plating and Six Weeks after Plating.

In addition to analyzing the grain size and internal stress of the tin deposits, SEM analysis was conducted after one day after plating to analyze surface morphology. The results are presented here as a function of deposition conditions. It is apparent from these photographs that duty cycle, frequency, current density and even hydrodynamic conditions have a strong influence on the morphology of the deposits. SEM photographs given in Figures 7-9 were taken at 3000X magnification. Figure 7 shows SEM photographs from PRC tests that utilize different test conditions. Figure 8 shows the effect of hydrodynamic flow for two DC tests run under the same current density.

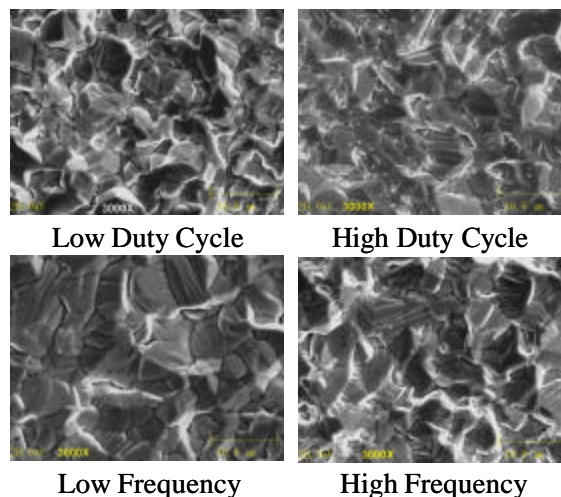


Figure 7. Effect of Wave form Parameters on Deposit Morphology for PRC Tests.

Figure 9 explores the effect of current density for both PC and PRC tests. The comparison of current density is not as straightforward as the previous comparisons. Figure 9 explores effect of current density and anodic pulse on the surface morphology; however, these may not be the only variables differing these tests. More tests need to be conducted to gain a better understanding of these relationships.

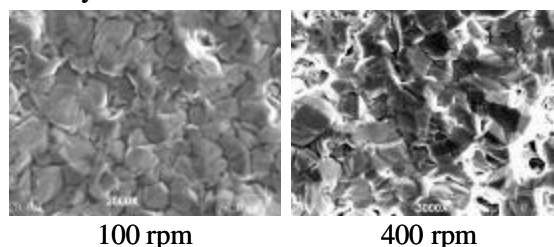


Figure 8. Effect of Hydrodynamic Flow on Deposit Morphology for DC Tests.

The propensity of each deposit to grow whiskers was also evaluated. None of the deposits showed signs of whiskering one day after plating through two months after plating. The coatings were not evaluated again for whiskers until after they had been aged for three years. All of the deposits showed signs of either whisker or hillock formation, observable with an optical microscope under 200X magnification. For some of these defects, it was not obvious whether the defects were a whisker or a hillock, due to the angle of microscope observation. The JEDEC standard does not consider or present standard methods for quantifying hillock growth. However, both whiskers and hillocks were photographed and documented for the current study.

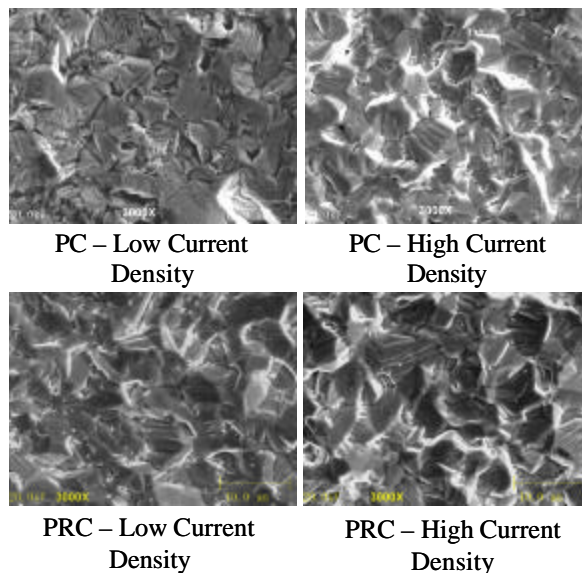


Figure 9. Effect of Current Density and Addition of Anodic Pulse for PC and PRC Tests.

Out of the twenty processes evaluated, two processes showed a significantly lower density of whisker/hillock growth, as well as significantly smaller sized defects as compared to the other processes. These two processes both utilized waveforms with a cathodic modulation followed by an off

time, a high frequency and a low duty cycle. The current density did not seem to have an effect; one test utilized the low current density while the other utilized the high current density. This is illustrated in Figure 10 and 11. Figure 10 shows the photographs from the two tests with the lowest density of whiskers/hillocks, for the densest areas on the coupons (the entire plated surface was analyzed for all coupons). The defects are circled, as they may be hard to see. Figure 11 illustrates photographs from the samples with the highest density of whiskers/hillocks and includes DC, PC and PRC tests.

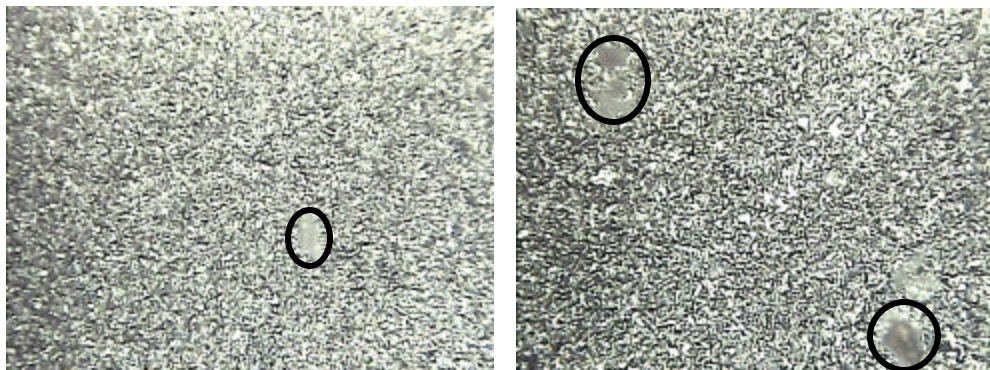


Figure 10. Optical Microscope Photographs of Pure Tin Electrodeposits with a Low-Density of Whiskers/Hillocks.

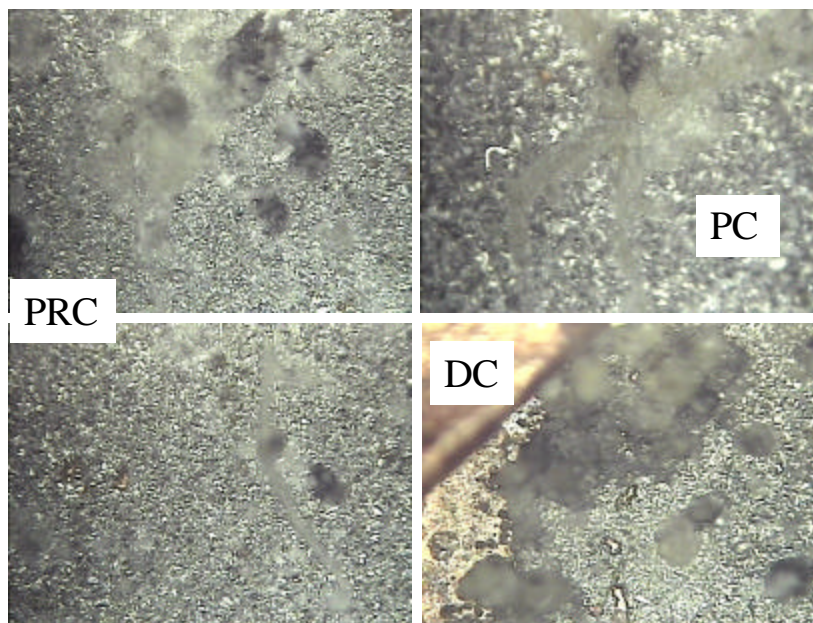


Figure 11. Optical Microscope Photographs of Pure Tin Electrodeposits with a High-Density of Whiskers/Hillocks.

Temperature Cycling Tests

The six different deposit “types” used for temperature cycling are outlined in Figure 4. These deposits were prepared by sequencing waveforms together to obtain the desired stratified stress coatings, in a single process step. Detailed evaluations of the deposits were performed by CALCE prior to temperature cycling tests. It was determined that many of the deposits suffered defects such as porosity issues, scratches in

the surface of the deposit presumably due to shipping and handling, uneven plating and other defects resulting from process inefficiency such as hydrogen bubbles erupting from the surface of the deposit causing defects, especially for Coating B. This demonstrates that the process is still under development, and further testing is required for process optimization.

The coupons were removed and inspected for whiskers after 500 cycles and then 1000 cycles and evaluated in terms of whisker density as well as average and maximum whisker length. Coupons prepared from a commercially available matte tin electroplating process were also tested for comparison purposes. The data from the temperature cycling tests is provided in Table II after 1000 cycles, at the conclusion of the test. Results from the samples prepared by the commercially available process are also listed in Table II. Faraday's samples are designated by FT-A through FT-F (per Figure 4) and the commercially available samples are designated by NC-14, NC-15 and NC-18. Note standard deviations for the commercial samples were provided but standard deviations from Faraday's test results were not; thus, Table II represents all data provided to Faraday. No whiskers were found on any of the FT samples after 500 cycles; data for the NC samples after 500 cycles was not provided.

Table II. Results from Temperature Cycling Tests for Samples Submitted by Faraday and a Commercial Vendor.

Sample	Density (#/mm ²)		Length (μm)		
	Av	STD	Av	STD	Max
FT-A	1		10		14
FT-B	1		14		46
FT-C	<1		15		24
FT-D	0		0		0
FT-E	0		0		0
FT-F	0		0		0
NC-14	45	35	5	4	13
NC-15	137	71	6	2	12
NC-18	16	1	3	2	7

From the temperature cycling results presented in Table II, it is interesting to note that the FT samples have a very low density of whiskers, if whiskers were found at all, compared to the density obtained from the commercially available (NC) samples. However, the average and maximum length of the whiskers observed were significantly higher in the samples submitted by Faraday as compared to the commercially available samples. The Coatings FT-D, FT-E and FT-F did not show signs of whiskering in the areas analyzed. These three coatings contained both compressive and tensile stresses, and could provide some insight into a strategy for whisker mitigation. SEM photographs of the longest whiskers observed for samples FT-A (Figure 12), FT-B (Figure 13) and FT-C (Figure 14) are provided below. As observed from Figures 14-16, the surfaces of the deposits were very rough. This is a further indication that this electrodeposition process needs optimization.

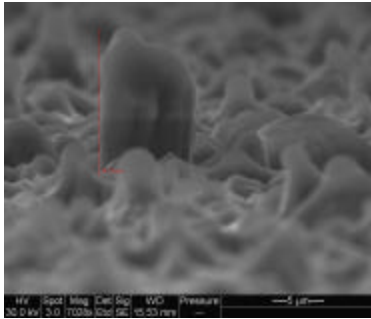


Figure 14. Longest Whisker (14 mm) Observed on FT-A after Temperature Cycling Tests.



Figure 13. Longest Whisker (46 mm) Observed on FT-B after Temperature Cycling Tests.

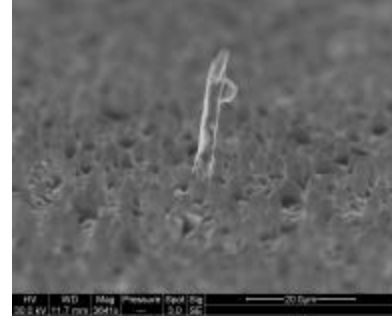


Figure 12. Longest Whisker (24 mm) Observed on FT-C after Temperature Cycling Tests.

Conclusions

The following work illustrates that electrically mediated deposition allows for tailoring of the properties of the pure tin deposits. Additionally, sophisticated coatings such as the stratified stress coatings can be achieved with sequenced waveforms from a single chemistry in a single process step. Some of these graded coatings showed better performance in the temperature cycling evaluations as compared to “pure tensile” deposits and a much lower density of whisker formation as compared to a commercially available matte plating process. When evaluating the deposits aged for three years, it was demonstrated that some electrically mediated processes, namely those utilizing a cathodic modulation followed by an off-time, a high frequency and a low duty cycle, show a lower propensity for whisker and hillock formation as compared to the other electrically mediated and DC processes. Work presented from the current study is on going; Faraday Technology is currently working on reproducibility studies, as well as *in-situ* stress measurements and high temperature/humidity (60°C/85% RH) storage tests for further process qualification.

Acknowledgments

This material is based upon work supported by a Small Business Innovative Research grant with the National Science Foundation, Grant No. OII-0450408. Any opinions, findings, and conclusions or recommendations expressed in this material are those of the authors and do not necessarily reflect the views of the National Science Foundation. The authors would also like to acknowledge Ms. Jenny Sun for Phase I experimental data and L. Panashchenko and S. Mathew from University of Maryland’s CALCE for SEM of deposits on brass coupons and temperature cycling data.

References

1. Y. Fukuda, S. Ganesan, M. Osterman and M. Pecht, "*Tin Whiskers in Electronics*", from Lead-free Electronics, S. Ganesan and M. Pecht Editors, Wiley-Interscience, Hoboken, NJ (2006).
2. J. Chang-Bing Lee, Y-L. Yao, F-Y. Chiang, P.J. Zheng, C.C. Liao, and Y.S. Chou, "Characterization Study of Lead-free SnCu Plated Packages," Proceedings of IEEE Electronic Component and Technology Conference, p. 1238-1245 (2002).
3. J.A. Brusse, G.J. Ewell, and J.P. Siplon, "Tin Whiskers: Attributes and Mitigation", CARTS EUROPE 2002: 16th Passive Components Symposium, Nice, France (2002).
4. K.N. Tu and J.C.M. Li, *Materials Science and Engineering A*, 409, p. 131-139 (2005).
5. J. Cl. Puipe, "*Influence of Pulse Plating on Crystallization*", Theory and Practice of Pulse Plating, J-C. Puipe and F. Leaman Editors, AESF, Orlando, FL, p. 17-39 (1986).
6. Y. Zhang and J.A. Abys, "*Tin and Tin Alloys for Lead-Free Solder*" in Modern Electroplating, M. Schlesinger and M. Paunovic Editors, Wiley Interscience, New York (2000).
7. A. Knodler, "*Pulsed Electrodeposition of Precious Metals*", Theory and Practice of Pulse Plating, J-C. Puipe and F. Leaman Editors, AESF, Orlando, FL, p. 119-175 (1986).
8. JEDCE Standard JESD22A121.01, "Test Method for Measuring Whisker Growth on Tin and Tin Alloy Surface Finishes", JEDEC Solid State Technology Association, Arlington, VA (2005).